Nuclear-spin echoes in GaAs:Zn and GaAs:In

D. Mao and P. C. Taylor
Department of Physics, University of Utah, Salt Lake City, Utah 84112
(Received 7 November 1994; revised manuscript received 15 May 1995)

We present a study of the spin echoes of ^{69}Ga, ^{71}Ga, and ^{75}As in GaAs single crystals with high concentrations of defects (1×10^{18} to 2×10^{20} cm^{-3}). The observed echoes have two distinctively resolved features: a rapidly decaying narrow component and a slowly decaying broad component. These two features correspond, respectively, to the broad satellite transitions and narrow central transition in the frequency domain. The satellite transitions are broadened by the quadrupolar interactions between the spins and the electric field gradients (EFG's) induced by defects. Defects produce the EFG's through lattice distortion (strain effect) and electric fields, if the defects are charged (charge effect). In order to separate these two effects, we used GaAs samples "doped" with indium or zinc. The widths and amplitudes of the echoes were investigated as functions of the orientation of the magnetic field and the defect concentration. We mapped the short-ranged strain field in terms of quadrupolar broadening of ^{69}Ga resonances. Within one lattice constant (a_0) from the defect, the strain-induced EFG's are so large that the satellite transitions are several MHz broad. At distances of a_0 to $\sim3a_0$ from the defect, the EFG's are large enough to spread out the satellite transitions from the central transitions. The satellite transitions of the nuclei in this region are undetectable in the free-induction decay. At distances of $3a_0$ to $\sim5a_0$ from the defect, the satellite transitions are only slightly broadened. At distances further away ($>5a_0$), the strain effect is negligible. For charged defects, in addition to the strain effect, EFG's are also produced by the electric fields through the perturbation of the valence electronic states. The charge effect is long ranged. The orientational dependence of the quadrupolar broadening is found to be in good agreement with earlier theoretical calculations, and the broadening is proportional to the defect concentration for defect concentrations as high as 10^{19} cm^{-3}. Finally, we point out that the earlier calculations of the defect concentration by the second-moment method were flawed because the strain effects were neglected.

I. INTRODUCTION

Nuclear magnetic resonance (NMR) has long been utilized to study the effect of defects in III-V semiconductors.[1–9] Local spin interactions, including the dipolar, pseudodipolar, exchange, and quadrupolar interactions, all perturb the Zeeman levels and contribute to the broadening of the NMR lines.[5] Among these interactions, the quadrupolar perturbation, which is the interaction between the quadrupole moments of the nuclei and the local electric-field gradients (EFG's), has received considerable attention because of its sensitivity to defects. In a perfect binary III-V alloy, all the lattice sites have tetrahedral symmetry and therefore zero EFG's. Defects in a crystal distort the lattice in many ways and induce nonzero EFG's. Information on the defect density, lattice distortion, etc. may be obtained by studying the quadrupolar broadening of the NMR lines.[5,9]

In a strong external magnetic field ($\mathbf{H}=H\hat{\mathbf{z}}$), the energy levels of the nuclear spins are mainly determined by the Zeeman interaction $E_m=m\hbar\gamma H$, $m=-I,-I+1,\ldots,I$, where γ and I are the gyromagnetic ratio and the spin of the nucleus, respectively, and m is the quantum number of the angular momentum S_z. Local spin interactions perturb the Zeeman levels slightly. The transition $(m=-\frac{1}{2})\Longleftrightarrow(m=\frac{1}{2})$ is called the central transition and the other transitions [e.g., $(m=-\frac{3}{2})\Longleftrightarrow(m=-\frac{1}{2})$] are called satellite transitions. Calculated to first order, the quadrupolar perturbation affects all the satellite transitions but not the central transition.

Roderick,[1,2] in his continuous-wave (cw) NMR studies of III-V semiconductors, observed that the NMR signal intensity decreased as the impurity concentration increased. He also noticed that charged defects were more "efficient" in producing the EFG's than isovalent "defects." Further investigations have been conducted by several researchers on GaAs with charged defects where carrier concentrations were below $\sim2\times10^{16}$ cm^{-3}.[4–8] In particular, Sundfors[4] and Hester *et al.*[5] examined the second moment of the resonance line as a function of the orientation of the crystal in a magnetic field; Fedders[6] and Cueman *et al.*[7] calculated the analytical form of the free-induction decay (FID), and Suemitsu and Nakajo[8] studied the analytical form of the spin echo. It is generally believed that the EFG's are mainly due to the distortion of the valence orbitals induced by the electric fields of the charged defects.[4–7] An elegant functional form for the orientational dependence of the second moment was calculated and was found in excellent agreement with experimental results.[5]

In the experiments mentioned above, samples with carrier concentrations less than 2×10^{16} cm^{-3} were used. The concentrations of charged defects could, in principle, be higher than the carrier concentrations if impurity compensation occurs, but neither the linewidths of the cw

spectra (2–3 kHZ) nor the decay times of the FID's ($T_2^* \sim 10^2$ μs) indicated that this was the case.[4,5] In these samples, the quadrupolar broadening was comparable in magnitude to other forms of broadening, and great effort was necessary to separate the individual contributions. As discussed by Hester *et al.*[5] and Cueman *et al.*,[7] the analysis tends to break down for samples with high defect concentrations. Even more disturbing, the defect concentrations calculated from the NMR data were more than an order of magnitude less than the actual carrier concentrations. In the present study, we would like to test the validity of the models in the regime where the defect concentration is above 1×10^{17} cm^{-3}. High defect concentration makes the quadrupolar broadening dominant and the other broadening mechanisms negligible. On the other hand, since the satellite transitions are significantly broadened, neither the cw NMR technique nor the FID technique is appropriate here. Therefore, we employ the spin-echo technique in this study.[10]

Lattice distortions due to isovalent defects have been studied by Carlos, Bishop, and Treacy.[9] Using GaAs samples with indium isovalent defects, these authors estimated the bond-angle distortions near the In atoms and the spatial extent of the strain field. Their analysis is mostly based on the fourier transform (FT) spectra and the assumption that the strain decreases as $1/r^3$, where r is the distance from the defect producing the distortion. In the case of large quadrupolar broadening, the FT spectra are not appropriate for measurements of the second moment of the line shape and the integrated signal intensity because the second-moment calculations are strongly affected by any baseline drift or phase error and the integrated signal intensities are strongly affected by incomplete spectral coverage of the satellite transitions. We will demonstrate that it is quite straightforward to measure the mean quadrupolar broadening in the time domain by studying the width and intensity of the echoes. Incidentally, the earlier works[5,7] on charged defects completely neglected the strain effects. We will show that this assumption is incorrect and is responsible for the discrepancy in the measurement of defect concentrations mentioned above.

II. EXPERIMENTAL DETAILS

The two GaAs:Zn samples used in this work have a zinc concentration of $\sim1\times10^{18}$ and $\sim2\times10^{19}$ cm^{-3} according to the specifications of the supplier (Sumitomo Electric Industries, Ltd.). They are labeled as ZN118 and ZN219, respectively, in the following discussion. The GaAs:In samples have indium concentrations of 1×10^{19}, 7×10^{19}, and 2×10^{20} cm^{-3} as determined by secondary-ion mass spectroscopy (SIMS).[9] They are labeled as IN119, IN719, and IN220, respectively. Concentrations of other defects (Si, B, Al, etc.) are all below 1×10^{16} cm^{-3}. The sample sizes are typically $5\times5\times0.3$ mm^3.

The relevant NMR properties of ^{69}Ga, ^{71}Ga, and ^{75}As are listed in Table I. Our focus will be on ^{69}Ga echoes, but ^{71}Ga and ^{75}As echoes will also be studied for comparison when necessary. The experiments were performed at room temperature on a standard NMR spectrometer at a magnetic field of 6 T. We use either the pulse sequence 90°-τ-64° to yield a maximum echo for spin-$\frac{3}{2}$ nuclei or the pulse sequence 90°-τ-110° to excite only the satellite transitions.[10] The highest possible rf power of our spectrometer typically gives a 90° pulse of about 2.5 μs for ^{69}Ga. Short rf pulses are essential to assure that the quadrupole echoes are not artificially broadened by the finite pulse width. A LeCroy digital oscilloscope (9400 A), which is capable of digitizing at a rate of 175 MHz, is used to acquire and average data. The spin-lattice relaxation times of the nuclei in our samples are typically 0.3 s at room temperature. It takes about 1.5 s for the excited spin system to fully relax to thermal equilibrium. Therefore, repetition rates faster than 1.5 s reduce the signal. On the other hand, rapid repetition increases the number of accumulations within a given period of time. As a compromise, a typical repetition rate of 0.5 s was used. Our discussion will concentrate on the time domain rather than the frequency domain for two reasons: (1) the satellites are stretched over a wide frequency range in the FT spectra and the diminished amplitude is difficult to study; and (2) in the case of quadrupolar nuclei, the second half of the echo is not exactly equivalent to the FID,[10] and therefore the FT spectrum of the echo is difficult to interpret.

III. RESULTS AND DISCUSSION

A. GaAs:Zn

In Fig. 1, we show ^{69}Ga spin echoes from ZN219 obtained under various experimental conditions. We first concentrate on the echo in Fig. 1(a), which is obtained using the pulse sequence 90°-τ-64° with the magnetic field (**H**) parallel to the (111) direction. It is apparent that there are two distinctive parts in the echo: a narrow component and a broad component.

The nature of the echoes can be understood by the following arguments. The NMR lines in III-V semiconductors are broadened by two basic types of local spin interactions: the electric quadrupolar interaction and the magnetic interactions, which include the dipolar, pseudipolar, and exchange interactions. In GaAs, the line

TABLE I. Nuclear properties.

Isotope	Natural abundance (%)	Spin (I))	Gyromagnetic ratio (MHz/T)	Electric quadrupole moment (rel)
^{71}Ga	40	3/2	12.984	1.0
^{69}Ga	60	3/2	10.218	1.6
^{75}As	100	3/2	7.292	2.0

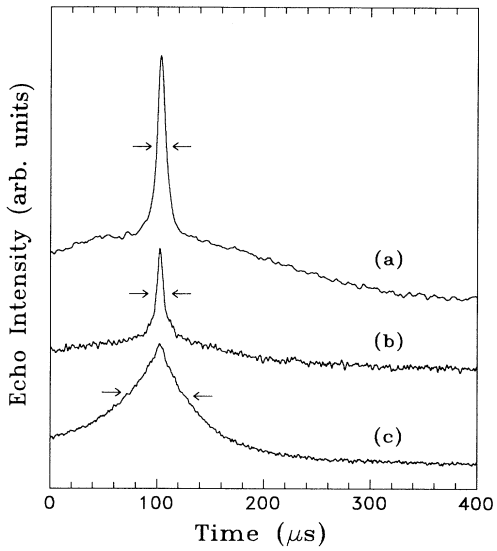

FIG. 1. ^{69}Ga spin echoes from ZN219. (a) $\mathbf{H}\|(111)$, 90°-τ-64° pulse sequence. The broad echo is from the central transition (the magnetic echo) and the narrow echo is from the satellite transition (the quadrupole echo). The width of the quadrupole echo is about 8 μs. (b) $\mathbf{H}\|(111)$, 90°-τ-110° pulse sequence. The magnetic echo is mostly suppressed while the quadrupole echo remains. (c) $\mathbf{H}\|(100)$, 90°-τ-110° pulse sequence. The quadrupole echo is much broader than that in (b). The full widths at half maximum of the quadrupole echoes are indicated by the arrows.

broadening due to the magnetic interactions is less than 5 kHz for all nuclear species. The quadrupolar broadening, however, is sensitive to the defect concentration (ρ_d); it is comparable to the magnetic broadening in magnitude for $\rho_d < 10^{17}$ cm^{-3} and dominant over the magnetic broadening for $\rho_d > 10^{18}$ cm^{-3}.[1,5] Calculated to first order as a perturbation on the Zeeman interaction, the quadrupolar interaction only broadens the satellite transitions but not the central transition. In samples like ZN118 and ZN219, the quadrupolar broadening is so large that the satellite transitions are spread out over a large frequency range and most of the intensity is easily separated from the central transition. The broad satellites appear in the time domain as a narrow echo (hereafter referred to as a quadrupole echo) and the narrow central transition appears as a broad echo (hereafter termed a magnetic echo).

The NMR frequency shift for a $(m \Longleftrightarrow m-1)$ transition, a, due to the quadrupole perturbation is given by

$$a = \frac{3(2m-1)eQ}{4I(2I-1)\hbar} V_{zz} ,$$

where Q and I are the electric quadrupole moment and the spin of the corresponding nucleus, and V_{zz} is the component of the EFG in the direction of $\mathbf{H}$. Obviously, a depends on the orientation of the EFG tensor with respect to $\mathbf{H}$. $eQ|V_{zz}|_{\max}/h$ is commonly defined as the quadrupole coupling constant, Q_{cc}. The mean quadrupolar broadening is defined as $w_Q = \langle a^2 \rangle^{1/2}$, where the average is over all nuclear sites. w_Q can be considered as the "half width" of the satellite transitions. If a Gaussian distribution function is assumed for a, the width of the quadrupole echo t_Q [full width at half maximum (FWHM)] is related to the mean quadrupolar broadening by a simple equation: $t_Q w_Q = 1.18$.[10] Clearly, a narrow quadrupole echo indicates a large quadrupolar broadening.

The quadrupole echoes of ^{71}Ga were also measured. The ratio of the quadrupolar broadenings for ^{69}Ga and ^{71}Ga is $w_Q(^{69}\text{Ga})/w_Q(^{71}\text{Ga}) = 1.5 \pm 0.2$, very close to the ratio of the quadrupole moments of the two isotopes $[Q(^{69}\text{Ga})/Q(^{71}\text{Ga}) = 1.6]$. This agreement confirms the assumption that the narrow echo is due to the satellite transitions.

By applying a 90°-τ-110° pulse sequence, we can suppress the magnetic echo and retain the quadrupole echo in order to measure accurately the width of the quadrupole echo. Figures 1(b) and 1(c) show such "pure" quadrupole echoes from ZN219 with $\mathbf{H}\|(111)$ and $\mathbf{H}\|(100)$, respectively. It is important to ensure that the widths of applied rf pluses are much narrower than the echo width to ensure accurate measurement of the echo width. Figure 2 shows the measured echo width as a function of the width of the 90° pulse. Data were taken on ZN219 with the magnetic field at an angle of 20° to a (100) axis. There is no artificial broadening when the 90° pulse width is narrower than $\frac{1}{3}$ of the echo width. On the other hand, when the 90° pulse is as wide as the echo, the measured echo width is about 50% broader than the true echo width.

It is apparent from Fig. 1 that the echo width depends on the orientation of the crystal with respect to $\mathbf{H}$. The rotation patterns were measured by rotating the crystal about a (110) axis, which was set perpendicular to $\mathbf{H}$. In Fig. 3, we show the mean quadrupolar broadenings (w_Q) of ^{69}Ga resonances for samples ZN219 [Fig. 3(a)] and ZN118 [Fig. 3(b)] as functions of θ, which is the angle between $\mathbf{H}$ and a (100) axis. As one would expect from the

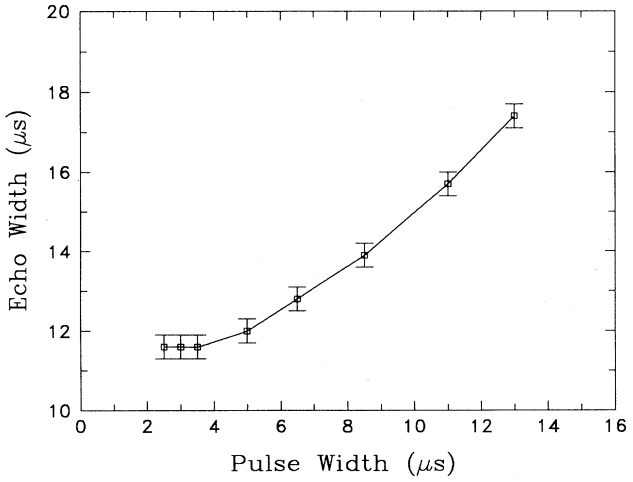

FIG. 2. Broadening of the spin echo by a finite rf pulse width. Data were obtained on the ZN219 sample as described in the text. The measured echo width is plotted as a function of the 90° pulse width. The solid line is a visual aid only.

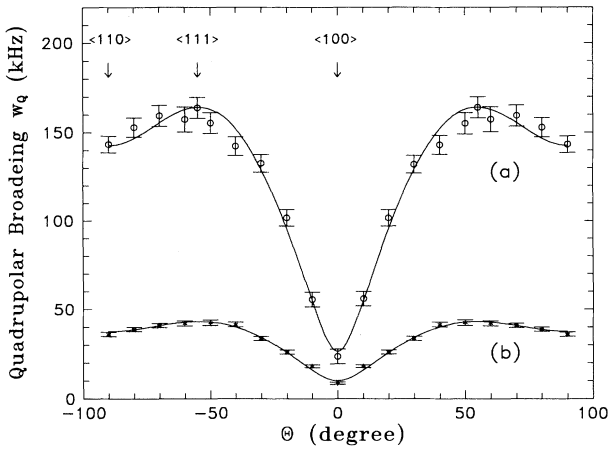

FIG. 3. Rotation patterns of w_Q for ^{69}Ga quadrupole echoes. (a) ZN219. (b) ZN118. The crystal is rotated about a (110) axis, which is perpendicular to **H**. θ is the angle in degrees between **H** and a (100) axis. The solid lines are fits of the data by the function $C+D(4\sin^2\theta-3\sin^4\theta)^{1/2}$ (see text for details). The arrows mark the three symmetry directions, (100), (111), and (110).

crystal symmetry, the results are independent of the particular (100) and (110) axes that were employed in taking the measurements. The rotation patterns are in excellent agreement with a model developed by Sundfors[4] and Hester *et al.*[5] In this model, the main contribution to the EFG is identified as the distortion of the valence-band wave functions by the electric field of the charged defect. In the coordinate system spanned by (100), (010), and (001), the EFG tensor (V_{ij}, $i,j=1,2,3$) and the components of the electric field E_i ($i=1,2,3$) are related by

$$V=R_{14}\begin{bmatrix}0 & E_3 & E_2\\ E_3 & 0 & E_1\\ E_2 & E_1 & 0\end{bmatrix}, \tag{1}$$

where R_{14} is a constant. Interestingly, all the diagonal elements of the EFG tensor are zero because of the tetrahedral symmetry of the lattice.

When the crystal is rotated about the (110) axis, the second moment ($\langle\Delta\nu^2\rangle_Q$) due to the quadrupolar interaction is given by[5]

$$\langle\Delta\nu^2\rangle_Q=\frac{6}{3}[4I(I+1)-3]\left[\frac{AR_{14}e^*}{\epsilon h}\right]^2\frac{\rho_d}{\rho}\times(4\sin^2\theta-3\sin^4\theta)\sum_j r_j^{-4}, \tag{2}$$

where $A=eQ/4I(2I-1)$, e^* is the effective charge of the defect, ϵ is the dielectric constant, ρ_d is the charged defect concentration, ρ is the nuclear density, and the summation is over the appropriate sublattice. While the exact relation between w_Q and $\langle\Delta\nu^2\rangle_Q$ is unknown, we expect $w_Q(\theta)$ to mimic the function $(4\sin^2\theta-3\sin^4\theta)^{1/2}$. In Fig. 3, we show fits of the rotation patterns $w_Q(\theta)$ of ZN219 and ZN118 using the function $C+D(4\sin^2\theta-3\sin^4\theta)^{1/2}$, where C and D are fitting parameters.

Unexpected from Eq. (2), the line broadening for $\mathbf{H}\|(100)$ (i.e., $\theta=0$), indicated by the parameter C in the fitting curves, is far from vanishing (about 9.4 kHz for ZN118 and 23.6 kHz for ZN219). This broadening has contributions from the isotropic part of the dipolar and exchange interactions.[5] However, as we shall see later in the discussion of GaAs:In, the major contribution is from the quadrupolar broadenings due to internal random strains, which are caused by the size difference between gallium and zinc atoms. Excluding $\theta=0$, the measured orientational dependence of the quadrupolar broadening is in agreement with the functional form described by Eq. (2). The parameter D is found to be proportional to $\rho^{0.5}$, as predicted from Eq. (2).

The rotation pattern of the ^{75}As echo is similar to that of ^{69}Ga. The mean quadrupolar broadening, however, is 1.7 ± 0.2 times that of ^{69}Ga in the same sample. This scaling is explained by the fact that the lattice summation $\sum_j r_j^{-4}$ has a larger value for the As sublattice than for the Ga sublattice. Intuitively, zinc atoms enter GaAs as accepters, substituting for Ga atoms. On average, As atoms are closer to zinc defects than Ga atoms and therefore experience larger EFG's. In addition, the Sternheimer factor for ^{75}As is slightly larger than that for ^{69}Ga. Sundfors found that the ratio of the Sternheimer factors for ^{75}As and ^{69}Ga is 1.1.[4]

The echo amplitudes are also orientationally dependent, as shown in Fig. 4. We studied the decay of the echo amplitude as a function of τ (separation between the two pulses) and found that the decay rates were different for different crystal orientations. Apparently, the variation in the echo intensities for a fixed τ simply reflects the difference in decay rates. This decay of the echo amplitude is due to homonuclear dipolar broadening, which is anisotropic and cannot be rephased by the spin-echo technique. From the decay rate, we can isolate the line broadening due to the homonuclear dipolar interaction.

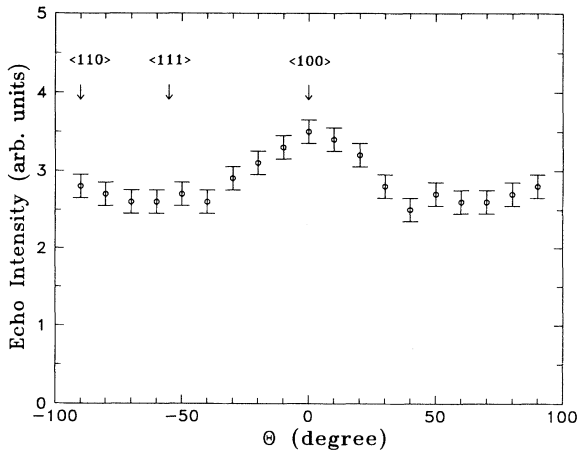

FIG. 4. The amplitude of the ^{69}Ga echo at $2\tau=1000$ μs as a function of θ for ZN118.

For instance, the echo decay rates are ~ 360 μs for $\mathbf{H}\|(111)$ and ~ 450 μs for $\mathbf{H}\|(100)$; assuming a Gaussian line shape, the homonuclear dipolar broadenings are then about 1.5 and 1.2 kHz for these two directions, respectively. These values can be checked against a rough estimate of the homonuclear dipolar interaction. The shortest Ga-Ga distance in GaAs is 4 Å, and the frequency shift due to the dipolar interaction between such a pair of spins ($\sim \gamma^2 h/r^3$) is about 110 Hz. For a Ga nucleus, there are 12 such nearest Ga neighbors, and therefore the total dipolar broadening from these nuclei can be on the order of 1 kHz.

B. GaAs:In

As in the case of GaAs:Zn, the echoes in GaAs:In consist of a narrow quadrupole echo and a broad magnetic echo. We employ the 90°-τ-110° pulse sequence to emphasize the quadrupole echoes. Rotation experiments similar to those shown in Fig. 3 indicate that the width of the quadrupole echo is independent of the crystal orientation. This fact implies that the EFG tensors are randomly oriented. Indium atoms enter the lattice by randomly substituting for the gallium atoms.[9] There is no net electric charge associated with these defects, but the lattice in the vicinity of the In atoms is distorted, or strained, to yield nonzero EFG's. Since this internal lattice strain propagates isotropically, the EFG tensors acquire a randomness.

The FWHM of the quadrupole echoes for IN119, IN719, and IN220 are 115±7, 21±15, and 9.8±0.5 μs, respectively. Figure 5 plots the quadrupolar broadening of ^{69}Ga as a function of the In concentration (ρ_{In}). The parameter w_Q increases sublinearly with ρ_{In}, $w_Q(^{69}\mathrm{Ga}) \propto \rho_{\mathrm{In}}^{0.84}$, in the investigated range of defect concentration. This empirical relation could be used to determine the In concentration of an unknown sample by measuring the quadrupolar broadening. By extrapolating the curve in Fig. 5 to $\rho_{\mathrm{In}} = 1.1 \times 10^{22}$ cm^{-3} (stoichiometric composition of $Ga_{0.5}In_{0.5}As$), we obtain a naive estimate of the quadrupolar broadening in the $Ga_{0.5}In_{0.5}As$ alloy: $w_Q(^{69}\mathrm{Ga}) \sim 3.0$ MHz. This rough estimation of the broadening also yields an estimate of the quadrupole coupling constant Q_{cc} of the Ga nuclei on the second nearest shell surrounding an In nucleus, $Q_{cc} \sim 2w_Q = 6$ MHz in $Ga_{0.5}In_{0.5}As$. For comparison, Carlos, Bishop, and Treacy[9] estimated Q_{cc} for the third nearest neighbors (As nuclei) to be 2.5 MHz.

Since the 90° pulse is about 2.5 μs in our experiment, the spectral coverage is about 800 kHz. The satellite transitions of the first few shells of neighbors of In atoms are likely to be undetected or at least not completely detected. This situation can be verified by examination of the FID amplitude and the echo amplitude. Figure 6 shows the FID's starting at 100 μs after the 90° pulse and the decays of the echo amplitudes for the three GaAs:In samples with $\mathbf{H}\|(100)$. We extrapolate the curves in Fig. 6 to $t = 0$ to find estimates of the initial amplitudes of the FID's and echoes, denoted by $A_{\mathrm{FID},0}$ and $A_{\mathrm{ECHO},0}$, respectively. The results are tabulated in Table II. In Table II, we also list $A_{\mathrm{FID,echo}}$, the initial FID amplitude calculated from the echo amplitude according to the equation $A_{\mathrm{FID,echo}} = A_{\mathrm{ECHO},0}/0.412$.[10] Two extreme cases are easily identified: if the quadrupolar broadening is smaller than the magnetic broadening, the $A_{\mathrm{FID},0}$ should include all the transitions (i.e., true FID amplitude $A_{\mathrm{FID},0}$); on the other hand, if the quadrupolar broadening is large enough to move the satellites out of the central transition, the $A_{\mathrm{FID},0}$ contains only the central transition and the true FID amplitude should be 2.5 $A_{\mathrm{FID},0}$. The factor 2.5 comes from the fact that the central transition contributes 40% of the total signal intensity while the satellites contribute 60%.

For the sample IN119, we find from Table II that $2.5\,A_{\mathrm{FID},0} > A_{\mathrm{FID,echo}} > A_{\mathrm{FID},0}$. This trend implies that the observed FID contains part of the satellite transitions,

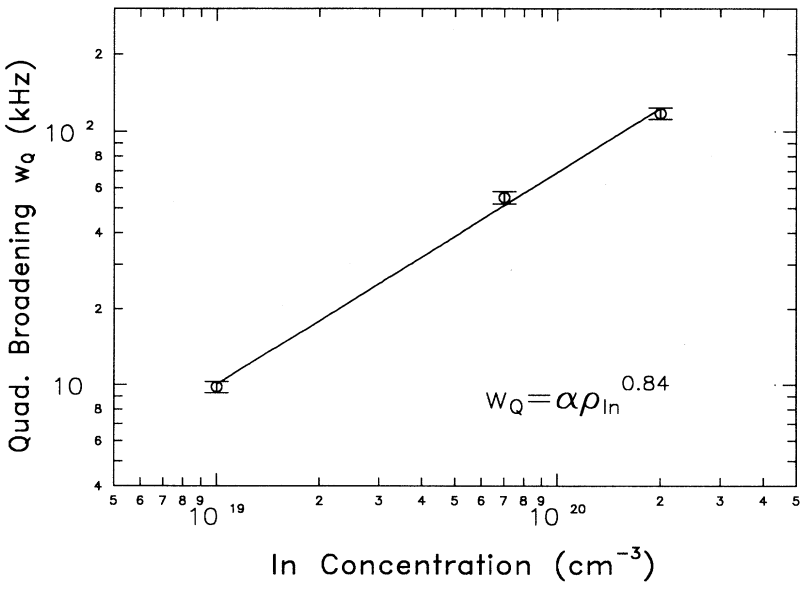

FIG. 5. The ^{69}Ga quadrupolar broadening in GaAs:In as a function of the In concentration. The solid line represents the function $w_Q(^{69}\mathrm{Ga}) \propto \rho_{\mathrm{In}}^{0.84}$. See text for details.

but not all. Let x be the fraction of the nuclei whose satellite transitions are significantly broadened and not detected in the FID, and $1-x$ be the fraction of nuclei whose broadened transitions are still detected in the FID. Using the data in Table II, we have the equation $410 \cdot x \cdot 1 + 410 \cdot (1-x) \cdot 0.4 = 285$. The solution is $x = 0.5$, i.e., about 50% of the nuclei have their satellite transitions well removed from the central transition. Note that the average In-In distance is 46 Å in this sample. In a simplified picture, we could say that strains at distances less than 18 Å ($\sim 3a_0$) from an In atom are large enough to make the satellite transitions of ^{69}Ga nuclei undetectable in the FID. Carlos, Bishop, and Treacy showed that the strain field is sufficient to affect the NMR of either the In or As nuclei at distances of about 30 Å ($\sim 5.3a_0$) from an In atom.[9] We conclude that at distances from $\sim 3a_0$ to $\sim 5a_0$ from an In atom, the satellite transitions are slightly broadened, but still detectable in the FID. For IN719, we have $A_{\mathrm{FID,echo}} = 277 \pm 21$ mV, very close to 2.5 $A_{\mathrm{FID},0} = 288 \pm 21$ mV, an indication that the FID contains only the central transitions. For sample IN220, we find that $A_{\mathrm{FID,echo}} = 170 \pm 13$ mV, also less than

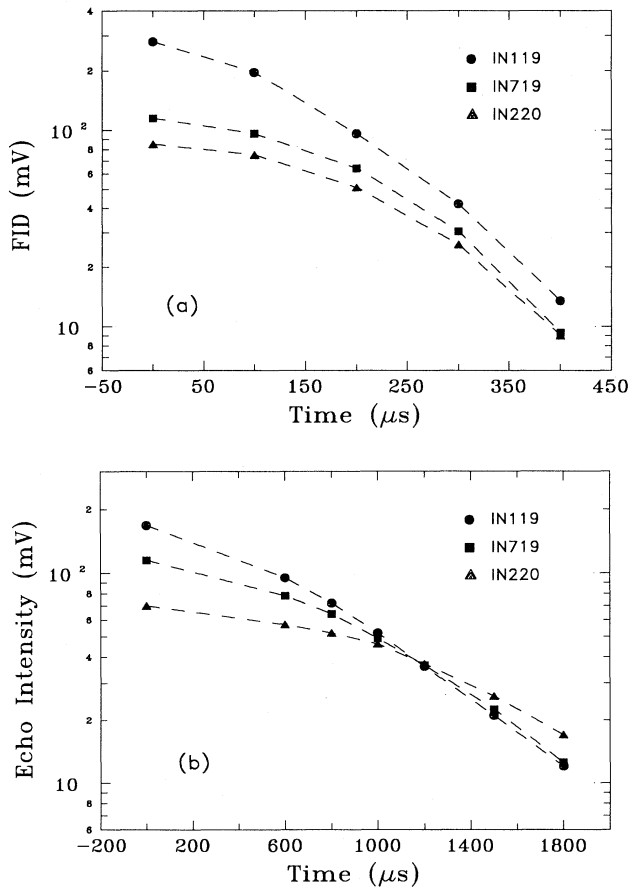

FIG. 6. Amplitudes of (a) FID's and (b) spin echoes from GaAs:In samples. Measurements of FID's start at 100 μs after the 90° pulse. The amplitudes of FID's and echoes at $t = 0$ are estimated by extrapolation of the corresponding curves and the results are tabulated in Table II.

TABLE II. ^{69}Ga signal intensities in GaAs:In.

ρ_{In} (10^{19} cm^{-3})	$d_{\mathrm{In\text{-}In}}$ (Å)	$A_{\mathrm{Echo},0}$ (mV)	$A_{\mathrm{FID,echo}}$ (mV)	$A_{\mathrm{FID},0}$ (mv)
1	46.4	170±13	410±31	280±21
7	24.3	115±9	277±21	115±9
20	17.1	70±5	170±13	85±6

$2.5 A_{\mathrm{FID},0} = 212 \pm 16$ mV. Clearly, all the satellites are very broad and moved out from the central transition in this sample. The fact that $A_{\mathrm{FID,echo}} < 2.5\ A_{\mathrm{FID},0}$ can only be explained by the loss of echo intensity from some of the satellite transitions due to very large quadrupole broadening for the few nearest neighbors of the In atoms. In fact, the echo signal is about 19% less than expected. For $\rho_{\mathrm{In}} = 2 \times 10^{20}$ cm^{-3}, each In atom is surrounded on the average by about 220 host atoms (Ga or As) and half of them are Ga. There are 12 and 6 Ga atoms, respectively, on the second and fourth nearest shells around an In atom. These nuclei represent $18/110 \approx 16\%$ of the total Ga atoms in IN220. It seems that these 18 Ga nuclei experience such large EFG's that their satellite transitions are beyond the spectral coverage in our experiments and are therefore undetected. Incidentally, the fourth nearest neighbors are at a distance of a_0 from the In atom. We point out that, in IN719, these shells of Ga atoms represent about 6% of the total Ga atoms and their effect may be unnoticed since our measurement is only accurate to about ±8%.

In earlier studies of charged defects, efforts were made to calculate the defect concentration from the measured second moment using Eq. (2). However, the calculated concentrations of defects were always an order of magnitude less than the carrier concentrations indicated by Hall-effect measurements.[5,7] The lack of agreement was attributed to the breakdown in the theory or to possible clustering of defects.[7] With the detailed knowledge about strain just acquired, we suggest that the discrepancy arises from the neglect of the strain effect in the earlier analyses. Defects, charged or neutral, inevitably produce strains in the lattice. While the defect-induced strain may vary in strength from defect to defect (likely depending on the size difference between the impurity atom and the host atom), it is almost certain that for the first few nearest neighbors of the defect, the strain-induced EFG's are so strong that the satellite transitions are undetectable in the FID. Correspondingly, in calculating the contribution to the second moment of the quadrupolar interaction [see Eq. (2)], the summation $\sum_j r_j^{-4}$ should exclude the contributions from the first few nearest neighbors of the defect. In the earlier analyses, however, the summations were taken over the entire lattice. Assuming that the strain induced by a zinc atom has similar strength to that induced by an indium atom, the appropriate summation should be performed only over lattice sites where $r > 3a_0$ since the satellite transitions of the nuclei at distances less than $3a_0$ from the charged defect are undetected in the FID. Our calculations show that the summation factor thus restricted is about one-tenth of the full summation factor. With the revised

summation factor, earlier calculations would have yielded correct defect densities. It is worth pointing out that nuclei within the strain sphere represent only 0.02% of the total nuclei for samples with a defect density of 1×10^{16} cm^{-3}. This tiny decrease in the FID intensity associated with the strain is unnoticeable.

IV. CONCLUSION

In summary, we have employed pulsed NMR to study the spin echoes of quadrupolar nuclei in GaAs crystals with high concentrations of charged defects (zinc) or isovalent "defects" (indium). The spin echo technique allows the detection of broader resonances than the cw NMR or FID technique. Analyses of the widths and intensities of echoes yield valuable information about the quadrupolar broadening of the resonances, which in turn tell about the EFG's induced by defects.

Defects produce EFG's in the lattice through two mechanisms: lattice distortion, or strain, and electric fields if the defects are charged. The strain effect is short ranged. We have obtained a detailed map of the EFG's induced by the strain. Within one lattice constant (a_0) from the defect, the strain-induced EFG's are so large that the satellite transitions are several MHz broad and undetectable even by the spin-echo technique. At distances of a_0 to $\sim3a_0$ from the defect, the EFG's are large enough to spread out the satellite transitions from the central transitions. The satellite transitions of these nuclei are undetectable in the FID. At distances of $3a_0$ to $\sim5a_0$ from the defect, the satellite transitions are only slightly broadened. At distances further away ($>5a_0$), the influence of strain is negligible. For charged defects, EFG's are also produced by the electric fields through the perturbation of the valence electronic states. The charge effect is long ranged. The orientational dependence of the quadrupolar broadening is found to be in good agreement with earlier theoretical calculations and the broadening is proportional to the defect concentration for defect concentrations as high as 10^{19} cm^{-3}. Finally, we have found the explanation to a twenty-year-old puzzle that the defect concentrations calculated from NMR data were often an order of magnitude less than the actual defect concentrations. The calculation of the second moment due to the charge effect should exclude contributions from the first few nearest neighbors of the defect ($r<3a_0$).

ACKNOWLEDGMENTS

We thank Sarah R. Kurtz of the National Renewable Energy Laboratory, and W. E. Carlos and T. Kennedy of the Naval Research Laboratory for generously providing the GaAs samples used in this work. This work was supported in part by the Office of Naval Research under Grant No. N00014-94-1-0941.

[1]E. H. Roderick, Philos. Mag. **3**, 545 (1958).
[2]E. H. Roderick, J. Chem. Phys. Solids **8**, 498 (1959).
[3]R. L. Mieher, Semicond. Semimet. **2**, 141 (1966).
[4]R. K. Sundfors, Phys. Rev. **185**, 458 (1969).
[5]R. K. Hester, A. Sher, J. F. Soest, and G. Weisz, Phys. Rev. B **10**, 4262 (1974).
[6]P. A. Fedders, Phys. Rev. B **11**, 1020 (1975).
[7]M. K. Cueman, R. K. Hester, A. Sher, J. F. Soest, and I. J. Lowe, Phys. Rev. B **12**, 3610 (1975).
[8]M. Suemitsu and N. Nakajo, J. Appl. Phys. **66**, 3178 (1989).
[9]W. E. Carlos, S. G. Bishop, and D. J. Treacy, Appl. Phys. Lett. **49**, 528 (1986).
[10]M. Mehring and O. Kanert, Z. Naturforsch. Teil A **24**, 768 (1969).